

NUMERICAL SIMULATIONS OF VICKERS INDENTATION CRACK GROWTH IN FERROELECTRIC SINGLE CRYSTALS: EFFECT OF MICROSTRUCTURE ON THE FRACTURE PROCESS

AMIR ABDOLLAHI AND IRENE ARIAS

Laboratori de Càlcul Numèric (LaCàN)
Departament de Matemàtica Aplicada III
Universitat Politècnica de Catalunya (UPC)
Campus Nord UPC-C2, E-08034 Barcelona, Spain
e-mail: irene.arias@upc.edu, <http://www-lacan.upc.edu>

Key words: Ferroelectricity, Fracture, Phase-field models, Finite element analysis

Abstract. The Vickers indentation technique is commonly used to investigate the fracture toughness of ferroelectric single crystals. Experiments show that the radial cracks perpendicular to the poling direction of the material propagate faster than the parallel ones. Using a phase-field model, we perform numerical simulations to show this anisotropy attributed to interactions between material microstructure and radial cracks. This model is based on a modified regularized formulation of the variational brittle fracture and domain evolution in ferroelectric materials.

1 INTRODUCTION

Ferroelectric materials exhibit strong electro-mechanical coupling which make them ideal materials for use in electro-mechanical devices such as sensors, actuators and transducers. To assure optimum reliability of these devices, understanding of the fracture behavior in these materials is essential. The complex nonlinear interactions of the mechanical and electrical fields in the vicinity of the crack, with localized switching phenomena, govern the fracture behavior of ferroelectric materials. Experimental techniques have been used to study fracture in ferroelectrics, including Vickers indentation to investigate the fracture toughness anisotropy [1–5]. Experiments show that cracking along the poling direction of the material has a shorter length and consequently a higher effective fracture toughness than that normal to the poling direction.

In this paper we introduce a model able to capture the anisotropic crack growth under Vickers indentation loading. This anisotropy is obtained by linking the crack propagation with the microstructural phenomena. The model treats in a coupled phase-field energetic

fashion both the brittle crack propagation and the microstructure evolution. We have recently presented a model, showing that the interaction of the microstructure and the crack leads to a slow-fast crack propagation behavior observed in experiment [6]. In Ref. [7], we have introduced a modification in the formulation to endow the phase-field model with the ability to simulate the aforementioned anisotropic crack growth. We present here the highlights of that work.

The theory of the coupled phase-field model is summarized in Section 2. Simulation results are presented and discussed in Section 3. The last Section is the conclusion of this paper.

2 PHASE-FIELD MODEL

The proposed approach to brittle fracture in ferroelectrics relies on the coupling of two energetic phase-field models, namely a time-dependent Ginzburg-Landau model for ferroelectric domain formation and evolution [8], and a variational regularized model of Griffith's fracture [9]. The electro-mechanical enthalpy density h is written as [6]

$$\begin{aligned}
 h(\varepsilon, \mathbf{p}, \mathbf{E}, v) &= (v^2 + \eta_\kappa) [U(\nabla \mathbf{p}) + W(\mathbf{p}, \varepsilon)] + W_e(\varepsilon, v) + \chi(\mathbf{p}) - \frac{\varepsilon_0}{2} |\mathbf{E}|^2 - \mathbf{E} \cdot \mathbf{p} \\
 &+ G_c \left[\frac{(1-v)^2}{4\kappa} + \kappa |\nabla v|^2 \right], \tag{1}
 \end{aligned}$$

where \mathbf{p} is the polarization, \mathbf{E} is the electric field defined as $\mathbf{E} = -\nabla \phi$, ϕ is the electrical potential, G_c is the critical energy release rate or the surface energy density in Griffith's theory and κ is a positive regularization constant to regulate the size of the fracture zone. The scalar field v provides a diffuse representation of the fracture zone, $v = 1$ and $v = 0$ indicating unbroken and broken material, respectively. The parameter η_κ is a small residual stiffness to avoid the singularity of the elastic energy in fully fractured regions of the domain. The domain wall energy density U , the electroelastic energy density W and the phase-separation potential χ in Eq. (1) are given in Ref. [7]. Note that here the energy functional W does not include the elastic energy and it is only associated with coupling terms between the strain and the total polarization \mathbf{p} . The elastic energy density W_e is written in [9] as

$$W_e(\varepsilon, v) = \kappa_0 \frac{\text{tr}^-(\varepsilon)^2}{2} + (v^2 + \eta_\kappa) \left(\kappa_0 \frac{\text{tr}^+(\varepsilon)^2}{2} + \mu \varepsilon_D \cdot \varepsilon_D \right), \tag{2}$$

where κ_0 and μ are the bulk and shear modulus of the material, respectively. The decomposition of the trace of the strain tensor ε in positive and negative parts are $\text{tr}^+ = \max(\text{tr}(\varepsilon), 0)$ and $\text{tr}^- = \max(-\text{tr}(\varepsilon), 0)$ and ε_D are the deviatoric components of the strain tensor. This decomposition is introduced to prevent crack nucleation, propagation and interpenetration in compressed regions by accounting for asymmetric behavior

in traction and compression. Note that here only the expansion and shear terms are multiplied by the jump set function $(v^2 + \eta_\kappa)$.

The stresses and electric displacements are derived from the electrical enthalpy as $\sigma = \partial h / \partial \varepsilon$ and $\mathbf{D} = -\partial h / \partial \mathbf{E}$. This particular formulation of the phase-field model encodes the traction-free, electrically permeable and free-polarization boundary conditions of a sharp-crack model [6].

The time evolution of the system results from the gradient flows of the total electro-mechanical enthalpy with respect to the primary variables v and \mathbf{p} , assuming that the displacement and the electric field adjust immediately to mechanical and electrostatic equilibrium (with infinite mobility), i.e.

$$\alpha \int_{\Omega} \dot{p}_i \delta p_i d\Omega = - \int_{\Omega} \frac{\partial h}{\partial p_i} \delta p_i d\Omega, \quad (3)$$

$$\beta \int_{\Omega} \dot{v} \delta v d\Omega = - \int_{\Omega} \frac{\partial h}{\partial v} \delta v d\Omega, \quad (4)$$

$$0 = \int_{\Omega} \sigma_{ij} \delta \varepsilon_{ij} d\Omega, \quad (5)$$

$$0 = \int_{\Omega} D_i \delta E_i d\Omega, \quad (6)$$

where $1/\alpha > 0$ and $1/\beta > 0$ are the mobilities of the processes. The weak form of the evolution and equilibrium equations is discretized in space with standard finite elements. Equations (3) and (4) are discretized in time with a semi-implicit scheme. A simple algorithm to solve the coupled system in a straightforward staggered approach is presented in Ref. [6].

3 NUMERICAL SIMULATIONS

We consider a rectangular domain with boundary conditions as shown in Fig. 1. The indentation is included in the model by considering a square inner boundary. The indentation faces are pulled by a monotonically increasing mechanical load w and electrical potential $\phi = 0$ is considered for these faces. The outer four edges of the simulated region are assumed to satisfy the following conditions: (1) $\sigma \cdot \mathbf{n} = \mathbf{0}$, (2) $\nabla \phi \cdot \mathbf{n} = 0$ and (3) $\nabla \mathbf{p} \cdot \mathbf{n} = \mathbf{0}$, where \mathbf{n} is the unit normal to the outer edges. The vertical initial polarization $\mathbf{p}_0 = (0, 1)$ is assigned to the sample in Fig. 1. The normalized dimensions of the domain are 200×200 ($L = 40$). The constants are chosen to fit the behavior of single crystals of barium titanate (BaTiO_3). The normalized constants are presented in Ref. [6]. The normalized critical surface energy density is chosen as $G'_c = 15.6$. Fifty load steps are computed with load increments of $\Delta w = 5 \times 10^{-2}$. The normalized time step $\Delta t' = 10^{-2}$ leads to convergent and accurate solutions for the time integration of gradient flow equations in Equations (3) and (4). The simulations are carried out using the finite element library of the Kratos multi-physics package [10].

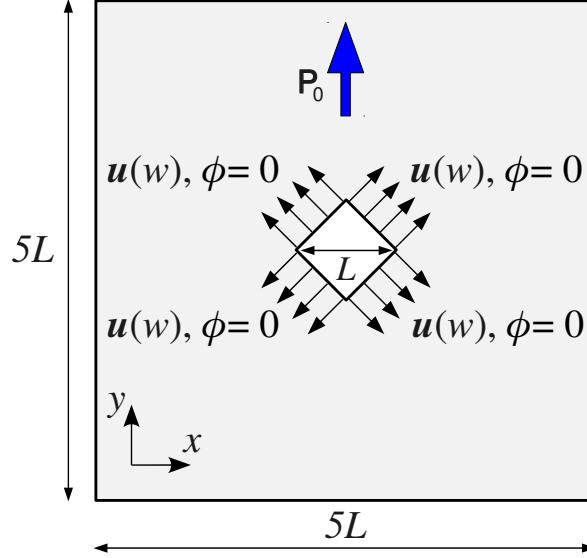


Figure 1: A schematic of the computational model.

Fig. 2 presents two snapshots of the crack propagation. The fracture zone grows along the four radial directions by increasing the load step as shown in two sample load steps $w = 1.5$ and $w = 2.5$.

The value of surface energy (integral over the domain of the last term in Eq. (1)) is obtained and presented in Fig. 3 for each of the four equal zones marked in Fig. 2(b). The surface energies of zones 1 and 3 follow nearly the same path. This also holds for zones 2 and 4. Interestingly, the surface energies of zones 2 and 4 are smaller than zones 1 and 3, i.e. the cracks propagating parallel to the polarization are shorter than those propagating perpendicularly. This is a clear evidence of the anisotropic crack propagation in agreement with experimental observations [1–5].

Fig. 4 presents the contours of polarization components in the load step $w = 1.8$. The x components of the polarization vectors indicate wing-shaped domains or twins around the tip of the parallel cracks in Fig. 4(a). This kind of ferroelastic domain switching is induced by the high tensile stresses near the crack tip which tend to elongate the material in the x direction in front of the parallel cracks. Since the polarization vectors are initialized in the direction of the tensile stresses near the perpendicular cracks, Fig. 4(b) does not show any twin formation around these cracks. Due to the absence of ferroelastic domain switching, the perpendicular cracks propagate longer than parallel ones and the fracture toughness is lower in the perpendicular direction to the initial polarization. The domain switching-induced toughening is also reported in other experiments of crack propagation in BaTiO_3 [11, 12].

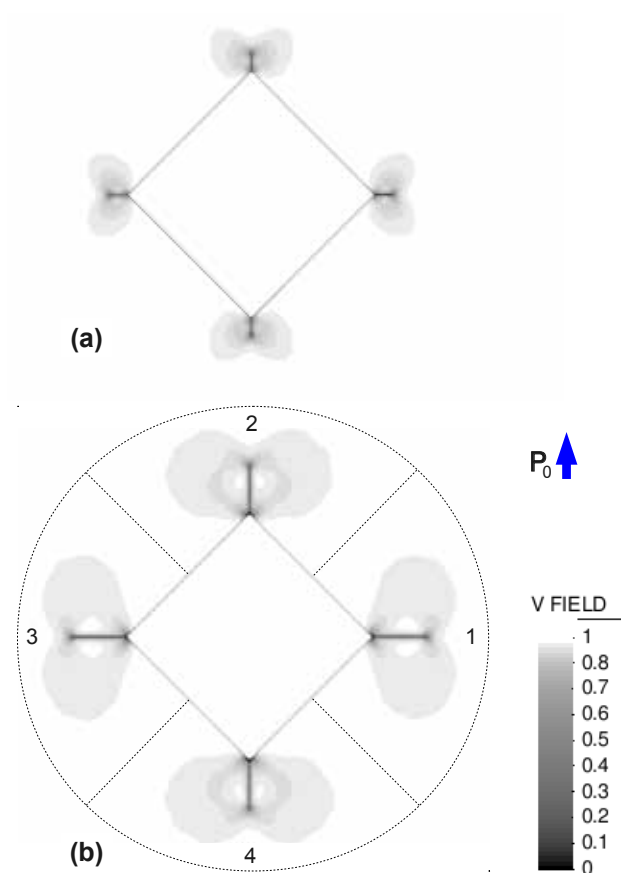


Figure 2: Contour plots of the field v for two snapshots of the fracture evolution at load steps (a) $w = 1.5$ (b) $w = 2.5$. Four equally large areas around the corners of the indentation are considered to obtain the surface energy evolution of the four radial cracks (zones 1 – 4) shown in Fig. 3.

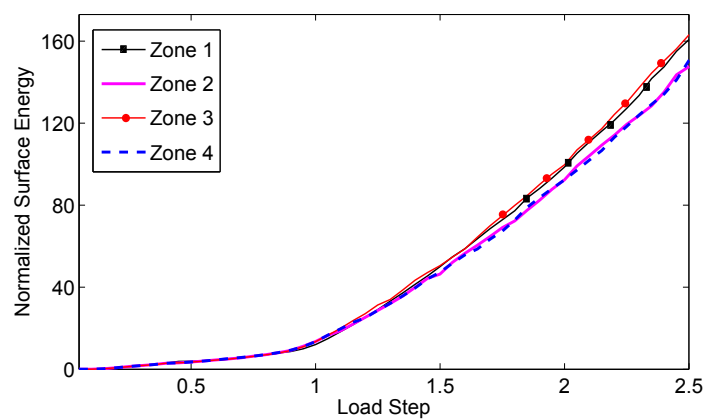


Figure 3: Evolution of the normalized surface energy of four zones as a function of the load step.

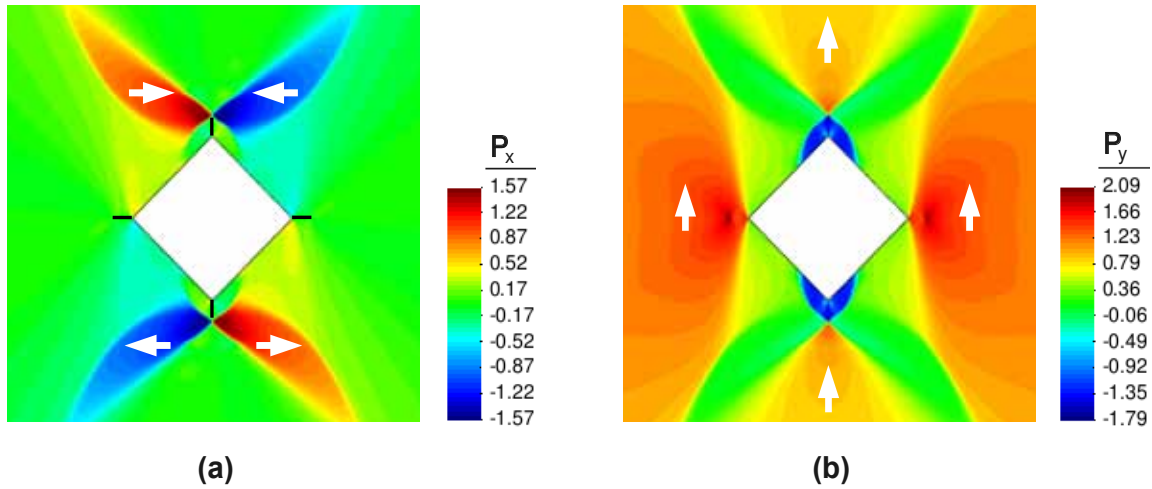


Figure 4: Distribution of polarization components in an area near the indentation in the load step $w = 1.8$ (a) x and (b) y components. Black lines in (a) indicate the position of the cracks ($v = 0$). Domain orientations are indicated with arrows.

4 CONCLUSIONS

We present a general formulation of coupled phase-field model based on variational formulations of brittle crack propagation and domain evolution in ferroelectric materials. Using this model, the simulation of Vickers indentation crack growth in ferroelectric single crystals is performed. The simulation results show that radial cracks parallel to the poling direction of the material propagate slower than perpendicular ones, which is in agreement with experimental observations. Ferroelastic switching induced by the intense crack-tip stress field is observed near the parallel cracks, which is believed as the main fracture toughening mechanism in ferroelectric materials.

References

- [1] Pisarenko, G.G., Chushko, V.M. and Kovalev, S.P. Anisotropy of fracture toughness of piezoelectric ceramics. *J. Am. Ceram. Soc.* (1985) **68**:259–265.
- [2] Tobin, A.G. and Pak, Y.E. Effect of electric fields on fracture behavior of PZT ceramics. *Proc. SPIE, Smart Struct. Mater* (1993) **1916**:78–86.
- [3] Wang, H.Y. and Singh, R.N. Crack propagation in piezoelectric ceramics: Effects of applied electric fields. *J. Appl. Phys.* (1997) **81**:7471–7479.
- [4] Lynch, C.S. Fracture of ferroelectric and relaxor electro-ceramics: Influence of electric field. *Acta Mater.* (1998) **46**:599–608.
- [5] Schneider, G.A. and Heyer, V. Influence of the electric field on vickers indentation crack growth in BaTiO₃. *J. Eur. Ceram. Soc.* (1999) **19**:1299–1306.

- [6] Abdollahi, A. and Arias, I. Phase-field modeling of the coupled microstructure and fracture evolution in ferroelectric single crystals. *Acta Mater.* (2011) DOI: 10.1016/j.actamat.2011.03.030.
- [7] Abdollahi, A. and Arias, I. Phase-field simulation of anisotropic crack propagation in ferroelectric single crystals: effect of microstructure on the fracture process. *Modelling Simul. Mater. Sci. Eng.* (2011), in press.
- [8] Zhang, W. and Bhattacharya, K. A computational model of ferroelectric domains. Part I: model formulation and domain switching. *Acta Mater.* (2005) **53**:185–198.
- [9] Amor, H., Marigo, J.J. and Maurini, C. Regularized formulation of the variational brittle fracture with unilateral contact: Numerical experiments. *J. Mech. Phys. Solids* (2009) **57**:1209–1229.
- [10] Dadvand, P., Rossi, R. and Onate E. An object-oriented environment for developing finite element codes for multi-disciplinary applications. *Arch. Comput. Methods Eng.* (2010) **17**:253–297.
- [11] Meschke, F., Raddatz, O., Kolleck, A. and Schneider G.A. R-curve behavior and crack-closure stresses in barium titanate and (Mg,Y)-PSZ ceramics. *J. Am. Ceram. Soc.* (2000) **83**:353–361.
- [12] Fang, D.N., Jiang, Y.J., Li, S. and Sun, C.T. Interactions between domain switching and crack propagation in poled BaTiO₃ single crystal under mechanical loading. *Acta Mater.* (2007) **55**:5758–5767.